

EXPERIMENTAL ANALYSIS OF VELOCITY FIELD STRUCTURE IN ISOTHERMAL COUNTERCURRENT JETS

BARBARA WOJCIECHOWSKA
PIOTR DOMAGAŁA
STANISŁAW DROBNIAK

Czestochowa University of Technology, Institute of Thermal Machinery, Poland
e-mail: bwoj@imc.pcz.czyst.pl

The paper presents results of experimental analysis of the flowfield in isothermal countercurrent round jets. The velocity measurements were carried out by means of a hot-wire anemometry. The instantaneous signals collected during the experiment were digitally processed and used to determine the statistics of velocity fields and distributions of turbulence scales. The results revealed that the fluid aspiration at the jet periphery significantly influences the mixing and entrainment in the free flow.

Key words: countercurrent jets, turbulence intensity, turbulence scales

Notations

- $(\cdot)_1$ – related to main jet (inner)
- $(\cdot)_2$ – related to aspirated reverse flow (outer)
- α – extension collar divergence half-angle
- Λ – linear Taylor macroscale
- λ – linear Taylor microscale
- ν – kinematic viscosity coefficient
- \overline{U} – local mean velocity
- \overline{U}_0 – mean reference velocity at the exit of the inner nozzle
- τ_t – correlation time distance
- D_1 – diameter of inner jet
- D_2 – diameter of outer jet
- I – ratio of the inner to outer velocity

L	–	extension collar length
$R(\tau)$	–	longitudinal velocity autocorrelation function
Re	–	Reynolds number based on D_1
T	–	time macroscale of turbulence
Tu	–	turbulence intensity u'/\bar{U}
U	–	local instantaneous velocity
u'	–	turbulence component of U_1 (RMS)
x	–	axial coordinate (attached to the exit plane of internal nozzle)

1. Introduction

The countercurrent jet is the subject of a number of publications which appeared mostly during the recent decade. The reason for this interest is twofold, i.e. the applicability of this type of flow in many practical technologies and the appearance of interesting flow phenomena like the absolute instability.

The first motivation for the research on counter-current jets, i.e. the enhancement of mixing was initiated by the experiment of Strykowski and Niccum (1991), who revealed the great potential of that way of flow stimulation in terms of intensification of transport processes. The phenomenon had a local character, i.e. intensive mixing took place in a limited space of the stream, and additionally was compensated by flow "laminarisation" (i.e. damping of turbulent fluctuations) in the remaining jet regions. However, the enhancement of mixing in the entire flow area could be obtained by control of the exit shear layer performed by application of extension tubes, as it was shown by Strykowski and Wilcoxon (1993). The research on counter-current jet control with extension tubes performed by Asendrych (2007) revealed that a substantial modification of large scale vortical structures was obtained in presence of a counterflow which, in turn, affected the mixing intensity. Summing up, careful control of this flow may allow for effective use of intensification of the mixing, and possible applications of this type of flow concern chemical processes and gas burners where the enhancement of mixing is of primary importance. An interesting perspective for application of counter-current jets was the substantial increase of diffusion flame blow-off limit shown by Lourenco *et al.* (1996) and confirmed by Asendrych and Frania (2004). Another special case for practical use of this flow configuration is the thrust vectoring in jet engines (Roy, 2001) where a countercurrent jet may be a new, more effective and more efficient way of the flow control.

The second motivation for investigations of counter-current jets is the appearance of absolute instability experimentally found in heated jets by Monkewitz *et al.* (1990) and in helium jets by Kyle and Sreenivasan (1993). The theoretical justification for absolute instability triggered by an external counterflowing jet was shown theoretically by Jendoubi and Strykowski (1994), but so far no convincing experimental evidence has been found for the existence of this phenomenon in counter-current jets. The extensive investigations of isothermal and heated counter-current jets performed by Asendrych (2000, 2007), Asendrych and Drobniak (2002), Asendrych and Favre-Marinet (2004), Bogusławski *et al.* (2002) could only reveal the existence of side jets and the substantial increase of jet spreading rate, which might suggest the appearance of absolute instability, which, however, could not be treated as a direct evidence (this problem still needs further investigations).

The motivation for the present study resulted from the research performed at ITM CzUT within the framework of TIMECOP EU project devoted to modelling of liquid fuel atomization and combustion in jet engines. The counter-current jet was selected as the test flow for investigations of fuel droplets evaporation (<http://timecop-ae.com/>) due to possibility of changing the structure of turbulence at the given point by changing the velocity ratio between the inner and outer jets. This unique feature of the counter-current jet is very convenient for experimental studies of droplet evaporation being performed by means of optical methods, which need careful alignment and, therefore, do not allow for easy traversing of measuring location. However, the analysis of experimental results published so far revealed the lack of data concerning the characteristic scales of turbulent motion, which are the basic parameters for studies of droplet evaporation (Birouk and Gokalp, 2006). This finding determined the goal of the present research, which was devoted to the experimental determination of turbulence scales in counter-current jets.

2. Experimental facility and measurements

The experiment was performed in an open-circuit wind tunnel equipped with a set of two concentric nozzles shown in Figure 1 and described in more detail in Asendrych (2007), Bogusławski *et al.* (2002). The main component of the test rig is an inner nozzle, which is made of brass. This nozzle generates an air stream with a very low turbulence level and "flat" profile of mean velocity at the exit of the inner nozzle. The roughness of the inner surface of the nozzle was carefully polished in order to avoid any possible disturbances generated

at the nozzle surface. Additionally, to enable control of the flow, an extension collar was mounted at the outer jet exit. Its additional aim was to reduce the influence of the back flow on the velocity field in the channel between the inner and outer nozzle.

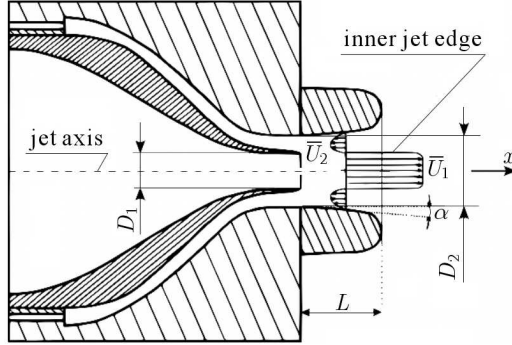


Fig. 1. The geometry of countercurrent nozzles (Bogusławski *et al.*, 2002)

The key parameter for the outer nozzle was the shape of the inner surface, because a very high contraction ratio (~ 128) had to be applied in order to maintain as low turbulence level as possible. The cubic profile of the inner nozzle enabled one to obtain an extremely low turbulence level at the inner jet exit, which was below the noise level of Constant Temperature Anemometer CTA. Additionally, the design of the outer nozzle allowed for replacement of orifices which determined the inlet width of the suction channel. The outer nozzle and the extension collar were made of aluminium. The geometry of these two nozzles is shown in Figure 1, the dimensions of nozzles applied in the experiment were as follows:

- inner diameter $D_1 = 15$ mm
- outer diameter $D_2 = 30$ mm
- extension tube height $L = D_1$
- divergence half-angle $\alpha = 7^\circ$.

The measurements of the velocity field were performed along the jet radius in several control planes covering the area $x/D_1 = 0 - 11D_1$ as well as along the inner jet axis and along the line being the extension of the edge of the inner nozzle. The measurements were performed with CTA which had to be precisely adjusted and aligned, which was possible in a given point only. The spreading rate of main stream could be changed by the parameter I , which was defined as the ratio of the inner-to-outer velocity. The main flow parameters of the reported experiment were as follows:

- Reynolds number $Re = \overline{U}_1 D_1 / \nu \approx 10000$ and 20000
- aspiration intensity expressed as the ratio of mean velocities of the reverse flow and main stream $I = \overline{U}_2 / \overline{U}_1 = 0 \div 0.4$.

The time scales of turbulence, i.e. Taylor micro and macroscales have been determined using the standard procedures described in Hinze (1975). The time microscale of turbulence τ_t can be expressed in terms of an autocorrelation function of longitudinal velocity fluctuations $R(\tau)$ with the following equation

$$\frac{1}{\tau_t^2} = -\frac{1}{2} \left[\frac{\partial^2 R(\tau)}{\partial \tau^2} \right]_{\tau=0} \quad (2.1)$$

where $R(\tau)$ is a symmetrical function of τ with the maximum value equal to unity for $\tau = 0$, and $R(\tau)$ decreases with increasing τ . The value of time turbulence microscale τ_t may be computed from the intersection of osculation parabola with τ axis as shown in Fig. 2.

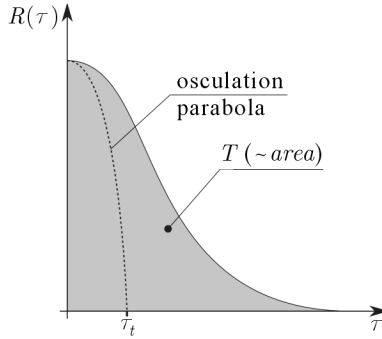


Fig. 2. Osculation parabola of the lateral correlation coefficient $R(\tau)$ and turbulent length scales τ_t and T

The time macroscale of turbulence T is given by the following equation

$$T = \int_0^{\infty} R(\tau) d\tau \quad (2.2)$$

The time micro- and macroscales of turbulence determined from the auto-correlation functions were transformed to linear scales with the use of Taylor hypothesis (Elsner, 1987)

$$\lambda = \overline{U}_1 \tau_t \quad \Lambda = \overline{U}_1 T \quad (2.3)$$

The measurements were carried out with the use of DANTEC single-channel hot-wire anemometer. The setup is shown schematically in Fig. 3.

The constant temperature anemometer was used to recover the instantaneous velocity of flow.

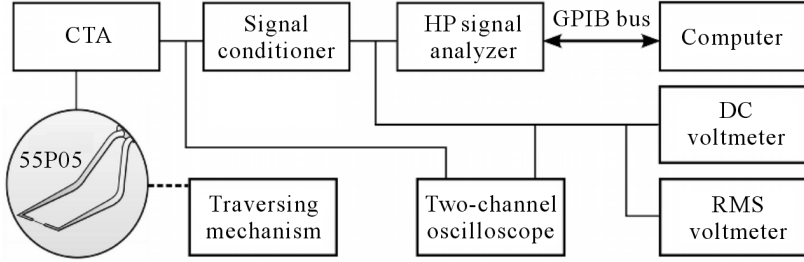


Fig. 3. Scheme of the measuring equipment

Velocity measurements were performed with DANTEC gold-plated wire probe 55P05. Instantaneous voltage signals of CTA were sent to the signal conditioners and data analysis system. In order to enable continuous monitoring of the experiment, all signals were visualized by oscilloscopes, and their average values were controlled by mean voltage meters. The signal processing, i.e. recovering the instantaneous velocity value U as well as evaluation of the statistical moments and spectral density functions, was performed fully digitally by an HP signal analyzer.

3. Characteristics of the flow field in isothermal countercurrent jets

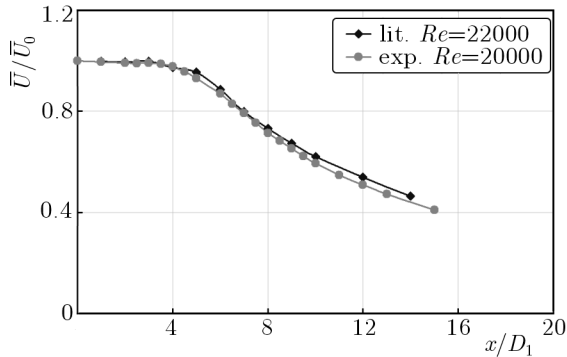


Fig. 4. Comparison of present experimental data for mean velocity with literature (Drobniak and Klajny, 2002) (measurements along the jet axis)

Figures 4 and 5 present the comparison of present experimental data for the mean velocity and turbulence intensity with the literature data (Drobniak and Klajny, 2002) for a similar Reynolds number along the symmetry axis of the jet (Drobniak and Klajny, 2002). The results for the mean velocity (Fig. 4) are in a very good agreement with the literature data. Also the data for the turbulence intensity (Fig. 5) are very similar except for the first region where some differences can be noticed. These differences are most probably due to much lower turbulence intensity at the jet exit obtained during the present experiment, which may be attributed to the corrected shape of the nozzle and better selection of gauzes in the plenum chamber.

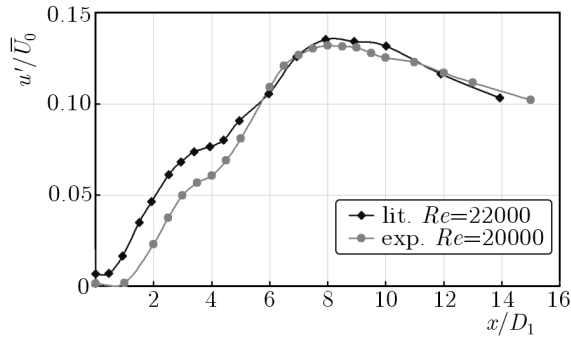


Fig. 5. Comparison of present experimental data for turbulence intensity with literature (Drobniak and Klajny, 2002) (measurements along the jet axis)

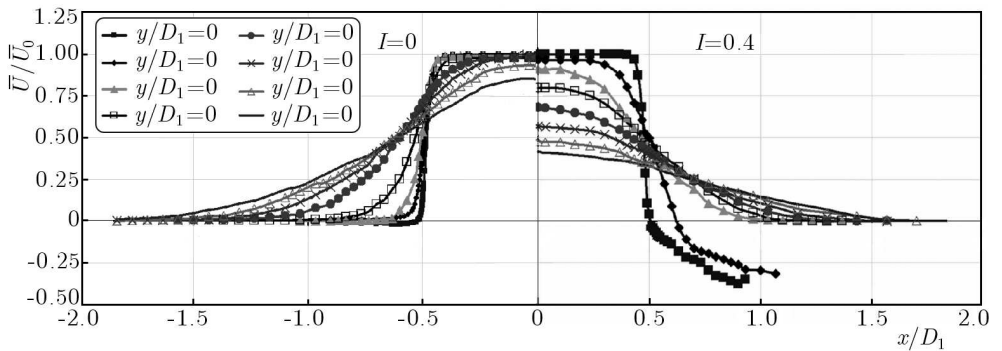


Fig. 6. Comparison of mean velocity radial distribution for different suction ratios for $Re = 10000$

In Fig. 6, one may observe the influence of suction ratio I on mean velocity profiles for $Re = 10000$. Velocity plots on the left hand side are for the suction ratio $I = 0$, and the plots on the right-hand side correspond to the case

of maximum suction $I = 0.4$. The case with no suction presents classical spreading of the jet with gradual decay of potential kernel. For the case with maximum suction the decay of potential kernel of the main jet is the most distinct influence. One may also notice the reversed flow in the first two cross-sections. The spreading rate for this case is smaller in the first cross-sections than in the reference case due to large suction intensity.

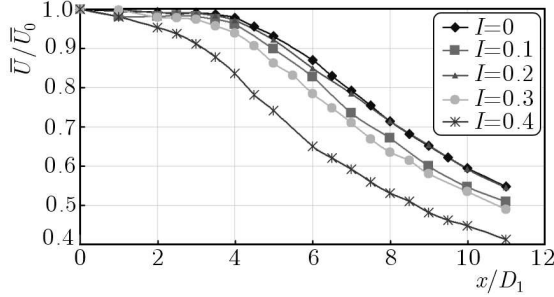


Fig. 7. Decay of mean velocity for $Re = 20000$ for various ratios of suction intensity I (measurements along the jet axis)

The change of flow parameters at the symmetry axis of the jet for $Re = 20000$ is shown in Figs. 7 and 8, both the decay of the potential core (Fig. 7) and the increase of turbulence intensity (Fig. 8) caused by suction are visible. These pictures present measurements obtained in consecutive cross-sections from the jet exit up to normalized distance $x/D_1 = 11D_1$. Both the mean velocity and RMS of velocity fluctuations have been normalized with the inner jet velocity \bar{U}_0 at the exit. The influence of suction is not monotonous, the smallest value of suction parameter $I = 0.1$ causes faster decay of the potential core and bigger increase of turbulence intensity than for $I = 0.2$. For larger values of I , the faster decay of mean velocity and increase of Tu is restored, for all values of I the maximum of Tu moves upstream. One may see that due to the change of variable I , the flow parameters change considerably at every point located at the jet axis. The decay of mean velocity at the jet axis for $Re = 20000$ is shown in Fig. 7 and for $Re = 10000$ in Fig. 9. The distance x and velocity \bar{U} are again normalized by the jet diameter D_1 and the inner jet velocity at the exit \bar{U}_0 . The same tendency is visible for both Reynolds numbers applied in present investigations for the mean velocity at the axis, but for lower Re the decay of the potential core is more conspicuous, and more monotonous decay of velocity caused by the increasing suction intensity is visible.

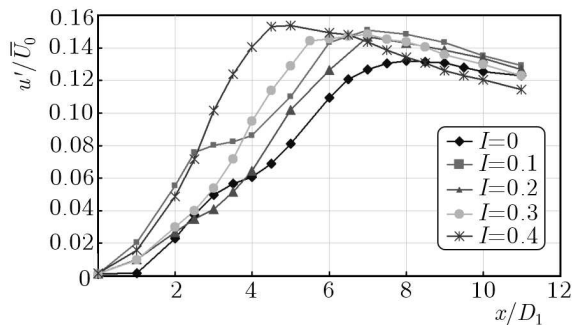


Fig. 8. Turbulence intensity evolution for $Re = 20000$ for various ratios of suction intensity I (measurements along the jet axis)

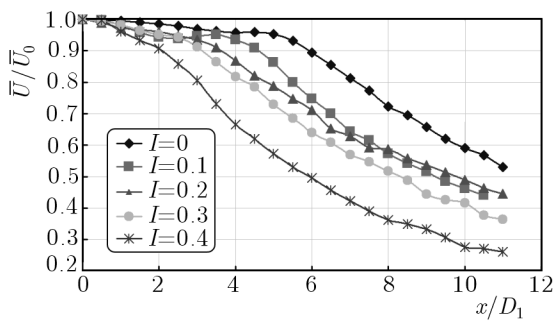


Fig. 9. Decay of mean velocity for $Re = 10000$ for various ratios of suction intensity I (measurements along the jet axis)

For the same two values of Reynolds numbers the evolution of turbulence intensity is shown in Figs. 8 and 10. Figure 8 presents data corresponding to $Re = 20000$, while Fig. 10 the data for $Re = 10000$. The comparison of Tu evolution along the jet axis reveals that for a lower Re number higher values of turbulence intensity and bigger increments of Tu for the same value of I were generally achieved. An other interesting observation is that the plateau of turbulence intensity, which was only slightly conspicuous for $I = 0$ and $Re = 20000$ at the distance $x/D_1 = 3 - 4D_1$ (Fig. 8), becomes much better visible for $I = 0.1$. This phenomenon was already reported by Drobnik and Klajny (2002) as related to vortex pairing, and for present investigations it may be of some importance as it changes the spectral content of turbulence in this region. The increase of outer-to-inner ratio stream parameter leads to even more perspicuous presence of this phenomenon. The maximum value $I = 0.4$ shifts the maximum of Tu much more upstream and allows one to expect even bigger modification of the spectral content of turbulence, which may be of some use in further investigations.

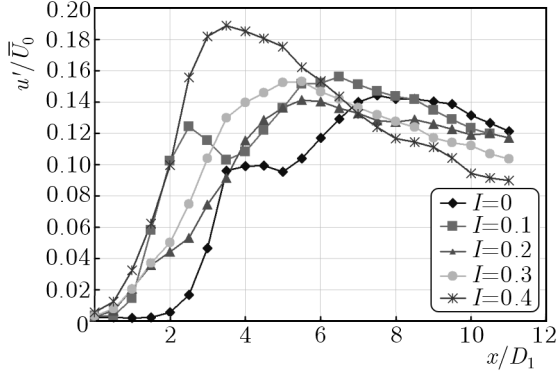


Fig. 10. Turbulence intensity evolution for $Re = 20000$ for various ratios of suction intensity I (measurements along the jet axis)

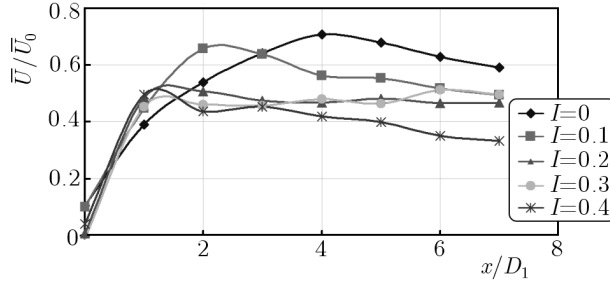


Fig. 11. Evolution of mean velocity for $Re = 10000$ and for various ratios of suction intensity I (measurements along the inner jet edge)

A summarised view on the influence of suction upon the velocity field along the jet edge is shown in Figs. 11 and 12 for $Re = 10000$. In Fig. 11, the distribution of mean velocity is presented, and in Fig. 12 the distribution of turbulence intensity is shown for all values of suction intensity which were applied in present investigations. The influence of suction upon the mean velocity field (Fig. 11) is more visible in the far region of the flow, while in the region close to the exit, the influence of suction is less visible.

The opposite effect is observed in the case of Tu intensity (Fig. 12), where suction exerts the biggest influence in the initial region of the flow, while in cross-sections from $x/D_1 = 5D_1$ all lines corresponding to various levels of suction almost collapse. One may notice that along this line one may achieve a very high value of turbulence intensity which reaches as high as $\sim 25\%$.

The next flow parameters which were of interest for present investigations were the scales of turbulence. Figures 13 and 14 present the downstream evolu-

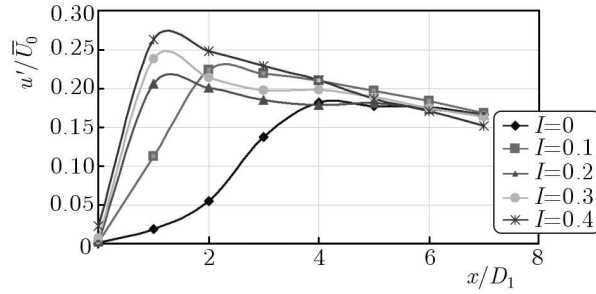


Fig. 12. Turbulence intensity evolution for $Re = 10000$ and for various ratios of suction intensity I (measurements along the inner jet edge)

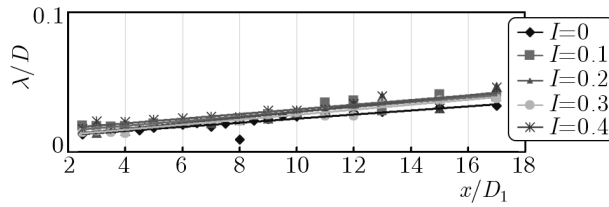


Fig. 13. Downstream evolution of linear Taylor microscale for $Re = 20000$ (measurements along the jet axis)

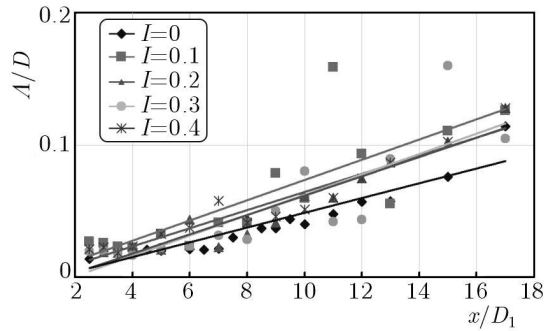


Fig. 14. Downstream evolution of linear Taylor macroscale for $Re = 20000$ (measurements along the jet axis)

tion of linear Taylor micro and macroscales for a sample value of $Re = 20000$ and for all values of the suction parameter. These results were obtained along the jet axis. One may notice that in the initial region, there is almost no difference between the micro- and macroscales, but it is not a surprise bearing in mind that the spectrum of turbulence did not develop here. As one moves downstream, both the micro- and macroscales increase, but the rate of increase for the macroscale is much faster, which confirms the well known rules of

increasing the frequency span with the development of turbulence. One may also notice that suction increases both the micro- and macroscale of turbulence, but the rate of increase of the macroscale is much faster, which reflects the widening of the spectrum of turbulence in the downstream direction. In Fig. 14, one should notice a substantial difference between the two measurements and the trend line. This discrepancy has been explained as resulting from the systematic error in two autocorrelation curves, and these points were not taken into account in calculation of the trend line.

4. Summary

The paper presents experimental study describing flow field characteristics in isothermal countercurrent round jets. The experiment confirmed that the reverse outer flow may substantially change the flow pattern of the inner jet proving that it can be utilised for active flow control. As the key parameter, the outer-to-inner flow ratio (the ratio of bulk velocities of the reverse stream and the main jet) was found with its critical value around 0.2. This tendency was visible for both Reynolds numbers applied in the investigations, but it proved to be more tangible for lower numbers Re . Another novel element of the paper is the presentation of the distribution of micro- and macroscales of turbulence, which to the best knowledge of authors has not been published so far.

Acknowledgements

The research was performed under the TIMECOP EU project (contract No. STREP 030828) and SPB TIMECOP funded by MNiSzW.

This work received funding from the European Community through the project TIMECOP-AE (Project # AST5-CT-2006-030828). It reflects only the author's views, and the Community is not liable for any use that may be made of the information contained therein.

References

1. ASENDRYCH D., 2000, Intensification of transport processes in free round co-current flows, *Ciepłne Maszyny Przepływowe, Turbomachinery*, **117**, II, 27-32

2. ASENDRYCH D., 2007, Active flow control by countercurrent jets, *J. of Theor. and Applied Mech.*, **45**, 3, 463-478
3. ASENDRYCH D., DROBNIAK S., 2002, Experimental analysis of the flowfield in non-isothermal countercurrent jets, *Advances in Turbulence*, **IX**, *Proc. 9th Eur. Turbulence Conf.*, Castro I.P. et al. (Edit.), 839
4. ASENDRYCH D., FAVRE-MARINET M., 2004, Diffusion of jets with annular counterflow and small diameter ratio, *AIAA Journal*, **42**, 11, 2385-2387
5. ASENDRYCH D., FRANIA T., 2004, Zastosowanie przepływu zwrotnego do optymalizacji spalania w strudze swobodnej, *XVI Krajowa Konferencja Mechaniki Płynów*, Waplewo
6. BIROUK M., GOKALP I., 2006, Current status of droplet evaporation in turbulent flows, *Progress in Energy and Combustion Science*, **32**, 408-423
7. BOGUSŁAWSKI A., ASENDRYCH D., DROBNIAK S., KUBACKI S., 2002, CFD simulations of concentric jets with external counterflow, *QNET-CFD Network Newsletter*, **1**, 3, 27-30
8. DROBNIAK S., KLAJNY R., 2002, Coherent Structures in Axisymmetric Free Jets, *J. of Turbulence*, **3**, 001
9. ELSNER J.W., 1987, *Turbulencja przepływów*, PWN Warszawa, ISBN 83-01-0613-4
10. HINZE J.O., 1975, *Turbulence*, McGraw-Hill Book Company, New York, ISBN 0-07-029037-7
11. JENDOUBI S., STRYKOWSKI P.J., 1994, Absolute and convective instability of axisymmetric jets with external flow, *Phys. Fluids*, **6**, 9, 3000-3009
12. KYLE D.M., SREENIVASAN K.R., 1993, The instability and breakdown of round variable density jet, *J. Fluid Mech.*, **249**, 619-664
13. LOURENCO L., SHEN H., KROTHAPALLI A., STRYKOWSKI P.J., 1996, Whole-field measurements on an excited premixed flame using on-line PIV, *8th Int. Symp. on Applications of Laser Techniques to Fluid Mech.*, Lisboa
14. MONKEWITZ P.A., BECHERT D.W., BARSIKOW B., LEHMAN B., 1990, Self-excited oscillations and mixing in a heated round jet, *J. Fluid Mech.*, **213**, 611-639
15. ROY G.D., 2001, Deflagrative and detonative combustion flows: reserch accomplishments and challenges in the new decade, *Proc. 5th ISAIIF*, Gdansk, Poland, 45-65
16. STRYKOWSKI P.J., NICCUM D.L., 1991, The stability of countercurrent mixing layers in circular jets, *J. Fluid Mech.*, **227**, 309-343
17. STRYKOWSKI P.J., WILCOXON L.G., 1993, Mixing enhancement due to global oscillations in jets with annular counterflow, *AIAA Journal*, **31**, 3, 564-570
18. <http://timecop-ae.com/>

Eksperymentalna analiza struktury pola prędkości w izotermicznych strugach przeciwbieżnych

Streszczenie

Artykuł przedstawia wyniki eksperymentalnej analizy pola prędkości izotermicznych strug przeciwbieżnych. Eksperyment przeprowadzony został z wykorzystaniem pionowego tunelu aerodynamicznego wyposażonego w układ dwóch dysz do generacji osiowosymetrycznych, koncentrycznych strug przeciwbieżnych. Pomiar prędkości został wykonany przy użyciu termoanemometrii. Uzyskane w trakcie badań wyniki pokazują, że zewnętrzna struga zwrotna ma istotny wpływ na rozwój wewnątrz strugi osiowosymetrycznej. Najistotniejszy parametr niniejszych badań, tzn. stosunek prędkości wewnętrznej i zewnętrznej strugi, wykazał wartość krytyczną $I = 0.2$. Prawidłowość tę zaobserwowano dla obydwu badanych liczb Reynoldsa, chociaż dla niższych liczb Reynoldsa tendencja ta była bardziej widoczna. Nowym elementem poznawczym było określenie rozkładu charakterystycznych skal turbulencji, które według wiedzy autorów nie były prezentowane w literaturze dla badanego przepływu.

Manuscript received April 16, 2008; accepted for print July 16, 2008